Characterization of the Ultrathin HfO_2 and Hf-Silicate Films Grown by Atomic Layer Deposition

Tze Chiang Chen, Cheng-Yi Peng, Chih-Hung Tseng, Ming-Han Liao, *Student Member, IEEE*, Mei-Hsin Chen, Chih-I Wu, Ming-Yau Chern, Pei-Jer Tzeng, *Member, IEEE*, and Chee Wee Liu, *Senior Member, IEEE*

***Abstract*—The physical properties of HfO_2 and Hf-silicate layers grown by the atomic layer chemical vapor deposition are characterized as a function of the Hf concentration and the annealing temperature. The peaks of Fourier transform infrared spectra at 960, 900, and 820 cm^{-1} originate from Hf–O–Si chemical bonds, revealing that a Hf-silicate interfacial layer began to form at the HfO_2/SiO_2 interface after postdeposition annealing process at 600 °C for 1 min. Moreover, the intensity of the peak at 750 cm^{-1} can indicate the degree of crystallization of HfO_2. The formed Hf-silicate layer between HfO_2 and SiO_2 is also confirmed by X-ray photoelectron spectroscopy.**

***Index Terms*—Fourier transform infrared (FTIR), HfO_2, Hf-silicate, high-k, X-ray photoelectron spectroscopy (XPS), X-ray reflectivity (XRR).**

I. Introduction

In ORDER TO meet the International Technology Roadmap for Semiconductor [1] requirements for equivalent oxide thickness (EOT) and gate leakage current, the conventional SiO_2 gate dielectric might need to be replaced by higher dielectric constant materials [2]. Using the "high-k dielectric" allows the device to maintain an EOT of 1 nm or less, while having a larger physical thickness to reduce the tunneling current. Among the various high-k dielectric materials, hafnium-based dielectrics are being widely investigated due to their high dielectric permittivity, high melting point, and acceptable thermal and chemical stabilities [3]–[6]. However, the hafnium-based dielectrics still have some critical issues, such as mobility degradation [7] and large flatband voltage shift [8], which impede their industrial application. Furthermore, it is hard to maintain the amorphous state for HfO_2 due to its low crystallization temperature (300 °C−400 °C) [9]. The pseudobinary materials, such as Hf-aluminate and Hf-silicate, combine the advantages of acceptable dielectric constant and desirable higher crystallization temperature [10]. Therefore, the material change of high-k dielectrics after the thermal process is a significant issue for the future CMOS applications. In this paper, we investigate the material and electrical modification of Hf-based dielectrics at different annealing conditions and different Si incorporations.

Manuscript received May 8, 2006; revised December 19, 2006. The work of the National Taiwan University group was supported by the National Science Council, Taiwan, R.O.C., under Contract 93-2215-E-002-003 and Contract 93-2215-E-002-017. The review of this paper was arranged by Editor G. Groeseneken.

T. C. Chen, C.-Y. Peng, and C.-H. Tseng are with the Department of Electrical Engineering and Graduate Institute of Electronics Engineering, National Taiwan University, Taipei 10617, Taiwan, R.O.C.

M.-H. Liao, M.-H. Chen, and C.-I Wu are with the Department of Electrical Engineering and Graduate Institute of Electro-Optical Engineering, National Taiwan University, Taipei 10617, Taiwan, R.O.C.

M.-Y. Chern is with the Department of Physics, National Taiwan University, Taipei 10617, Taiwan, R.O.C.

P.-J. Tzeng is with the Electronics Research and Service Organization, Industrial Technology Research Institute, Hsinchu 310, Taiwan, R.O.C.

C. W. Liu is with the Department of Electrical Engineering, Graduate Institute of Electronics Engineering, and Graduate Institute of Electro-Optical Engineering, National Taiwan University, Taipei 10617, Taiwan, R.O.C. (e-mail: chee@cc.ee.ntu.edu.tw).

Digital Object Identifier 10.1109/TED.2007.892012

II. Experiment

The high-k films were on the 15–25 $\Omega \cdot$ cm p-type Si wafers. All samples were treated with an SC-1 preclean process before high-k dielectrics deposition. This cleaning process typically results in a chemical oxide layer between high-k dielectrics and the Si substrate to enhance initial growth of the high-k dielectrics. The HfO_2 and Hf-silicate films were deposited by hot-wall atomic layer chemical vapor deposition [11] with a reaction temperature of 300 °C, using alternating surface-saturation reactions of $HfCl_4$, $SiCl_4$, and H_2O. Note that Hf-silicate films with different Hf/Si ratios ($Hf_{0.38}Si_{0.62}O_2$, $Hf_{0.5}Si_{0.5}O_2$, and $Hf_{0.66}Si_{0.34}O_2$) were grown using alternated nanomixed HfO_2/SiO_2 [12]. After deposition, a silicon nitride cap to form a thin passivation layer (< 0.5 nm) was deposited at 600 °C for 10 s using NH_3 and $SiCl_4$ precursors. The samples were annealed in the furnace at 600 °C for 1 min and 1000 °C for 5 min in N_2 ambient for postdeposition annealing (PDA). The furnace was kept at the atmospheric pressure and purged by nitrogen. The electrical properties were studied using metal–insulator–semiconductor (MIS) capacitors with a 50-nm-thick Pt electrode deposited by E-gun and a circular area of 2.5×10^{-4} cm^2 defined by the shadow mask. Another Al contact is deposited on the back of the sample. The postmetallization annealing (PMA) was done in forming gas, $N_2(90\%) + H_2(10\%)$, at 400 °C for 30 min before the electrical measurement. Fourier transform infrared (FTIR) spectroscopy was used to observe transmission spectra of the different chemical bonds and the change of bonding state after thermal processing. Each spectrum was measured with a resolution of 4 cm^{-1} and a range of 370–1800 cm^{-1} and transformed from transmission

0018-9383/$25.00 © 2007 IEEE

Authorized licensed use limited to: National Taiwan University. Downloaded on February 13, 2009 at 00:47 from IEEE Xplore. Restrictions apply.

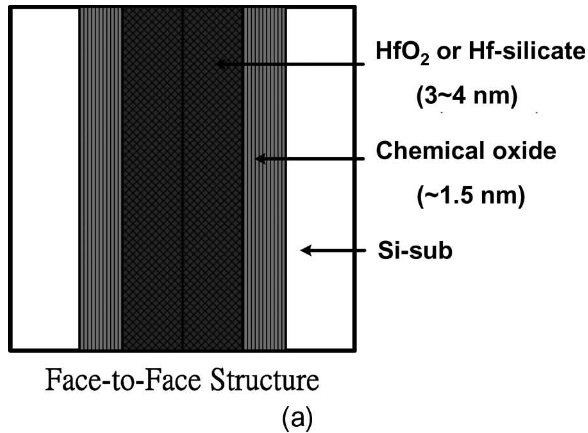

(a)

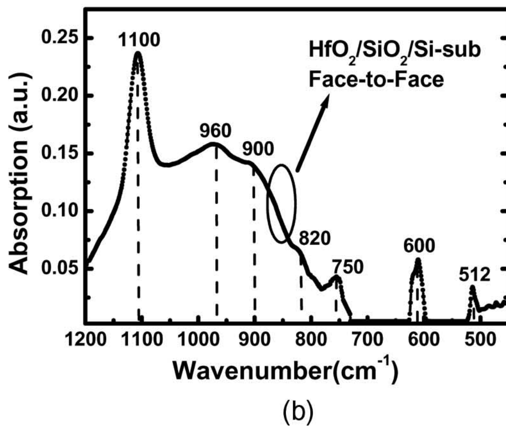

(b)

Fig. 1. (a) Scheme of FTIR measurement structure. (b) FTIR spectra of HfO_2 after PDA at 600 °C for 1 min in flowing N_2 measured by "face-to-face" structure. The intensity of IR signal with ultrathin high-k layer can be enhanced by the "face-to-face" method.

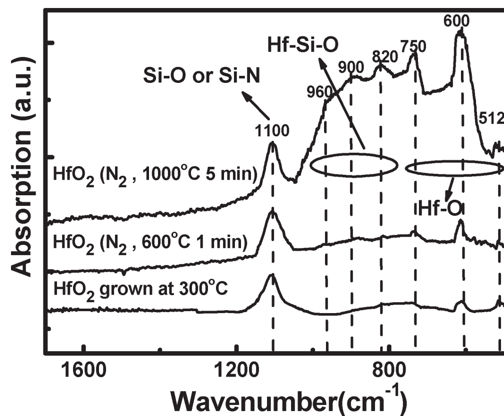

Fig. 2. FTIR spectra of ultrathin HfO_2 films as-deposited, annealed at 600 °C for 1 min, and annealed at 1000 °C for 5 min in N_2 ambient. The positions of the peaks in the three curves are indicated by dashed lines. The intensity of the peak at 750 cm^{-1} is clearly seen to increase the thermal budget.

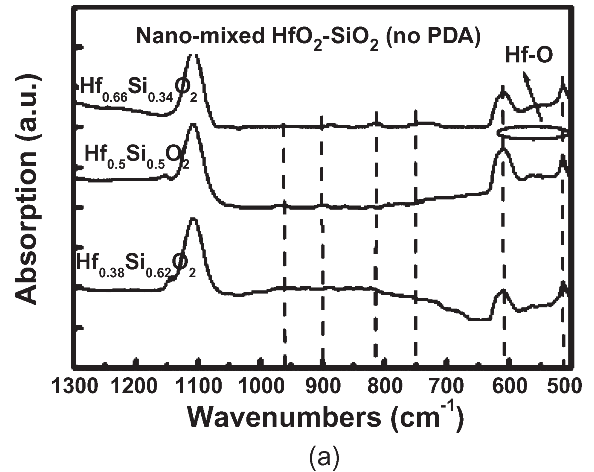

(a)

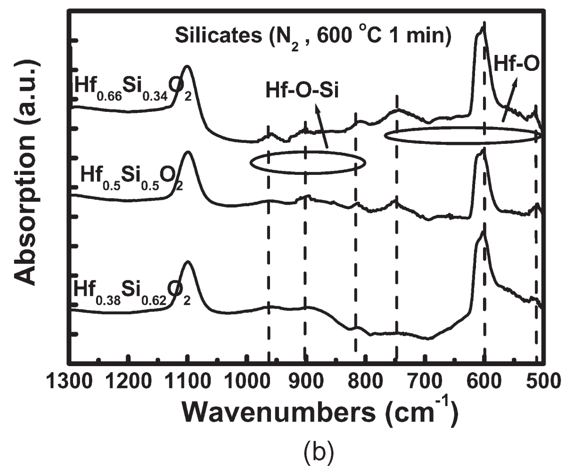

(b)

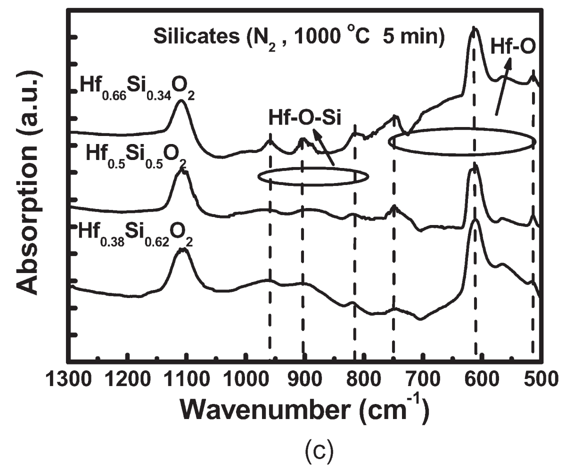

(c)

Fig. 3. FTIR absorption spectra of Hf-silicate. The samples in (a) were not annealed, and in (b) and (c), the samples were annealed in N_2 ambient for 1 min at 600 °C and for 5 min at 1000 °C, respectively. There are only two peaks (at 600 and 512 cm^{-1}) in the as-deposited nanomixed HfO_2/SiO_2, indicating no Hf-silicate formation.

to absorption. High-resolution transmission electron microscope (HRTEM) and X-ray photoelectron spectroscopy (XPS) were used for physical thickness inspection and observation of the chemical composition of the gate dielectrics. X-ray reflectivity (XRR) using $CuK\alpha$ source was used to study the constituent thickness and roughness of these films. The thickness obtained by XRR was calibrated with HRTEM measurements for layer thickness and atomic force microscopy (AFM) for surface roughness. The electrical properties of HfO_2 and Hf-silicate films on chemical oxide with different PDA conditions were also studied. The capacitance–voltage (C–V) and current–voltage (I–V) characteristics for electrical properties were measured with HP 4284A and Keithley 4200 instruments, respectively.

Authorized licensed use limited to: National Taiwan University. Downloaded on February 13, 2009 at 00:47 from IEEE Xplore. Restrictions apply.

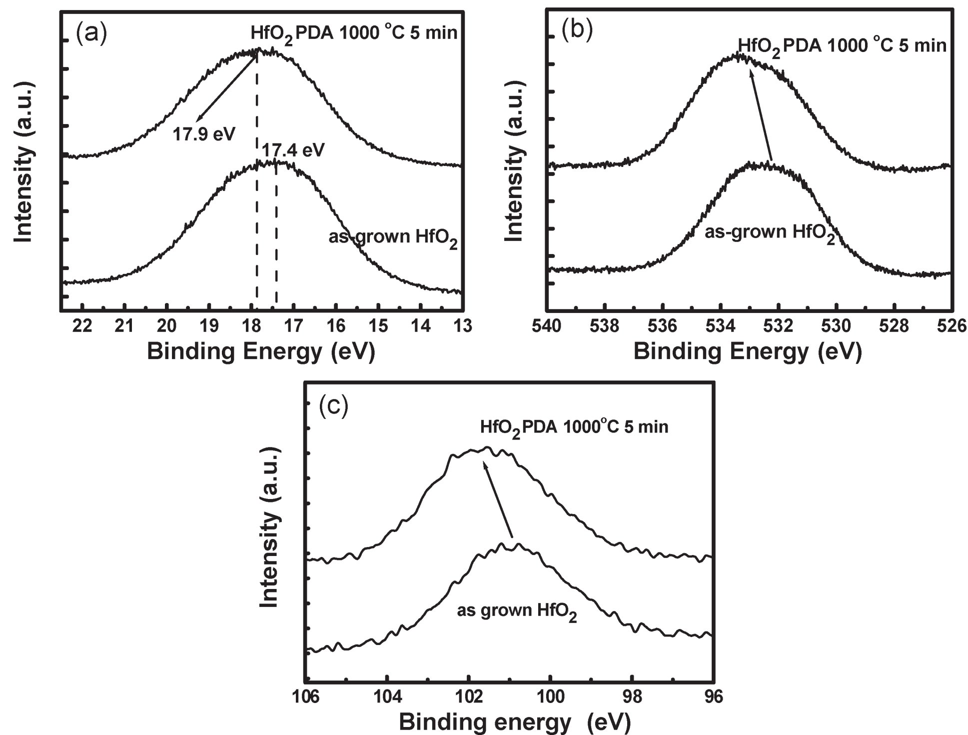

Fig. 4. XPS results of the (a) Hf 4f, (b) O 1s, and (c) Si 2p peaks for HfO_2 films as-grown and annealed at 1000 °C for 5 min in N_2 ambient. The shift of the Hf 4f, O 1s, and Si 2p peaks to higher binding energy is due to the formation of a Hf-silicate layer.

III. Results and Discussion

A. FTIR Results

FTIR analysis is a reliable and powerful method due to its convenient, rapid, and nondestructive measurement. However, the high-k gate dielectrics are too thin to detect in FTIR measurement, and the characteristics of a thin HfO_2 layer may be quite different from those of a thick one due to the crystallization [13]. Previous work has shown that it is possible to detect the chemical bonding vibrations of SiO_2, HfO_2, and hydrogen defects in layers as thin as several nanometers using attenuated total reflection and multiple internal reflection measurements [14]–[16]. Those techniques use a complicated method to adjust the incident angle of the IR beam to enhance the signal. A simple method to detect the weak signal from the ultrathin film and from the interface between the high-k layer and the oxide is reported here. A schematic cross section of our "face-to-face" measurement structure is shown in Fig. 1(a). The absorption is enhanced in the "face-to-face" structure due to the doubling of the film thickness and the reflection at the interface between the surfaces of two samples. Note that there is no observable absorption signal if we use only one sample in our measurement system. Fig. 1(b) shows the FTIR spectra of HfO_2 after annealing at 600 °C for 1 min by the "face-to-face" measurement structure. Fig. 2 shows the FTIR spectra of the as-deposited HfO_2 sample and the HfO_2 samples annealed at 600 °C (1000 °C) in N_2 ambient for 1 min (5 min). There are three peaks, at 750, 600, and 512 cm^{-1}, attributed to the Hf–O chemical bonds in the spectra, and the peaks at 960, 900, and 820 cm^{-1} are assigned to Hf–O–Si stretching vibrations [17]–[19]. The peak at around 1120 cm^{-1} may result from the absorption by the Si–N bond [20] formed by surface nitridation or from Si–O–Si bond absorption in the chemical oxide layer. The as-deposited HfO_2 film spectrum exhibits peaks at 600 and 512 cm^{-1} due to Hf–O chemical bonds, and these two peaks increase with annealing temperature, so does the 750 cm^{-1} peak. The intensity of the 750 cm^{-1} peak increases with the thermal budget of the HfO_2 due to the increasing degree of crystallization [21]. Comparing the three spectra (as-deposited, annealed at 600 °C, and annealed at 1000 °C), the intensities of the peaks at 960, 900, and 820 cm^{-1} are seen to increase with the thermal budget. This is due to the Hf–O–Si chemical bonds formed at the HfO_2/SiO_2 interface. The formation of silicate cannot be avoided during the thermal process. During the annealing process, Hf-silicate is formed by the atomic diffusion mechanism [22]. As a result of Si diffusion into HfO_2, the Hf-silicate should be formed in the original HfO_2 layer, thus increasing the interfacial layer thickness. The silicate interfacial layer shows no obvious contrast with the initial chemical oxide in the transmission electron microscopy (TEM) image (Fig. 5), indicating that the interfacial silicate might be Si rich. In Fig. 3, the FTIR absorption spectra of Hf-silicate are shown as a function of Hf concentration at different thermal annealing conditions. In Fig. 3(a), the as-deposited samples show no apparent peaks from 700 to 1000 cm^{-1}, which indicates that the as-deposited nanomixed HfO_2/SiO_2 does not intermix, whereas the peaks at 600 and 512 cm^{-1} are detected in as-deposited nanomixed HfO_2/SiO_2, indicating Hf–O bond formation. The annealing at 600 °C and 1000 °C generates absorption peaks due to Hf–O–Si stretching vibrations [Fig. 3(b) and (c)], indicating the intermixture and formation of Hf-silicate after the thermal annealing of the nanomixed

Authorized licensed use limited to: National Taiwan University. Downloaded on February 13, 2009 at 00:47 from IEEE Xplore. Restrictions apply.

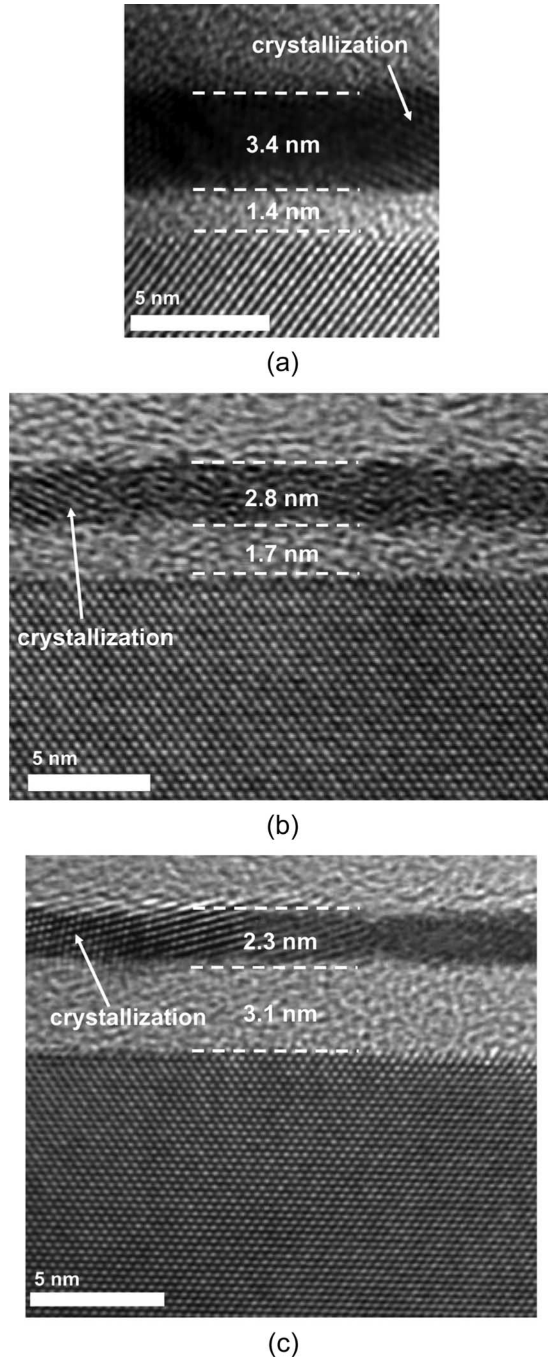

Fig. 5. HRTEM cross-sectional images of HfO_2 (a) as-deposited, (b) after 600 °C/1 min/N_2 annealing, and (c) after 1000 °C/5 min/N_2 annealing. The thickness of the interfacial layer between HfO_2 and Si is increased by annealing.

HfO_2/SiO_2. Moreover, the intensity of the peak at 750 cm^{-1} also increases the Hf concentration in Fig. 3(b) and (c), indicating slight occurrence of phase separation and crystallization at the high Hf concentration [23]. Due to the variation in each measurement, in Fig. 3, the intensity of oxide has been normalized. The integration of the Hf–O–Si peak area is only studied as a function of temperature in the $Hf_{0.66}Si_{0.34}O_2$ samples. The ratio of this sample with PDA at 600 °C for 1 min and PDA at 1000 °C for 5 min is 2, which indicates the increase of Hf–O–Si bonds with the increase of temperature. Note that,

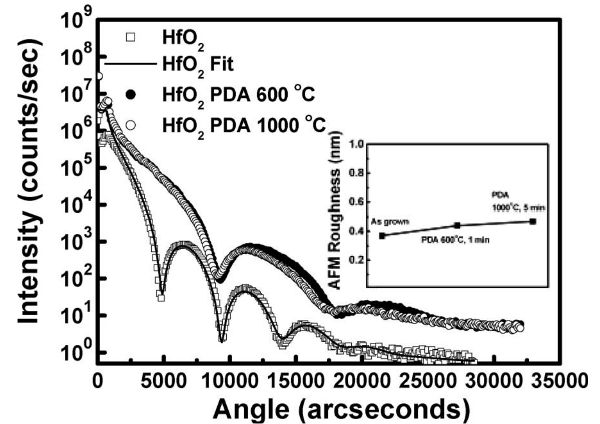

Fig. 6. XRR spectra of HfO_2 film as-deposited, after 1-min annealing in N_2 at 600 °C, and after 5-min annealing in N_2 at 1000 °C. The inset is the surface roughness for HfO_2 samples by AFM. The roughness of the HfO_2 surface is lower than 0.5 nm even after high-temperature annealing.

although the HfO_2 sample seems to have more pronounced Hf–O–Si peak (Fig. 2) than the nanomixed HfO_2/SiO_2 samples [Fig. 3(c)], the integration of the Hf–O–Si peak area (filtering the background of the broad signal) is slightly lower than the nanomixed HfO_2/SiO_2 samples. The quantitative analysis of the FTIR signal is not obtained by the difference of the optical alignment and environmental condition for each measurement.

B. Structural Analysis

The HfO_2 film on SiO_2 following PDA at 1000 °C is also characterized by XPS measurements, as shown in Fig. 4. In Fig. 4(a), the peak of the XPS of HfO_2 after the PDA process is at about 17.9 eV. The shift of Hf peak to higher binding energy is attributed to the formation of Hf-silicate film, which is 0.5 eV higher than that of the as-grown HfO_2 film (17.4 eV). Note that the two peaks (Hf $4f_{7/2}$ and Hf $4f_{5/2}$) of XPS in Hf element cannot be distinguished due to the limit of resolution of the XPS equipment. Furthermore, the O 1s spectrum [Fig. 4(b)] and Si 2p spectrum [Fig. 4(c)] of the annealed samples are also shifted to higher energy as compared to those of as-grown sample, indicating a strong signature of Hf-silicate formation. The intensity of reflected X-ray is dependent on the surface and near-surface electron density. Consequently, XRR has been used to study a variety of surface and thin film properties. In order to understand the effects of the PDA process, it is important to realize the effect on the chemical reaction at interface and the growth of the interfacial layer due to the increasing thermal budget. XRR and TEM have been utilized to analyze the physical characteristics of as-grown and postannealed HfO_2. The TEM images of HfO_2 thin films as-deposited, annealed at 600 °C for 1 min, and annealed at 1000 °C for 5 min are shown in Fig. 5(a), (b), and (c), respectively. Fig. 5(a) shows that the as-grown HfO_2 partially crystallizes only after 600 °C for 10 s for the Si_3N_4 cap. The degree of crystallization of HfO_2 is clearly increased when the sample was annealed at 1000 °C, which is also indicated by the peak at 750 cm^{-1} in Fig. 2. The thickness of the interfacial layer between the HfO_2 and the Si substrate increases with the thermal budget. Evidently, the HfO_2 film is partially consumed by the interfacial

Authorized licensed use limited to: National Taiwan University. Downloaded on February 13, 2009 at 00:47 from IEEE Xplore. Restrictions apply.

TABLE I
DETAILS OF THE XRR MODEL SIMULATED DATA AS COMPARED TO TEM AND AFM RESULTS

As grown			PDA 600°C 1min			PDA 1000°C 5 min	
Simulation (model 1)		TEM	Simulation (model 2)		TEM	Simulation (model 2)	TEM
SiO_2 (T)	1.3 nm	1.4 nm	SiO_2 (T)	1.7 nm	1.7 nm	3.5 nm	3.6 nm
HfO_2 (T)	3.4 nm	3.4 nm	Hf-silicate (T)	0.7 nm	2.8 nm	0.8 nm	2.3 nm
			HfO_2 (T)	2 nm		1.8 nm	
Density (D)	HfO_2 : 8.2 g/cm^3		Hf-silicate :	3 g/cm^3		3.2 g/cm^3	
			HfO_2 :	8.4 g/cm^3		8.4 g/cm^3	
Surface Roughness (R)	0.41 nm (XRR) 0.37 nm (AFM)		0.42 nm (XRR) 0.44 nm (AFM)			0.46 nm (XRR) 0.47 nm (AFM)	

silicate, since the HfO_2 thickness decreases after annealing. Note that the Si_3N_4 cap is not visible in the TEM picture, which may be due to the poor contrast between Si_3N_4 and the TEM bonding glue or too thin thickness of the Si_3N_4 cap. Fig. 6 depicts the XRR response of the HfO_2 film before and after thermal annealing. The period of oscillation in the XRR plot depends on the thickness of the layer with the highest electron density, which is HfO_2 in our samples. The HfO_2 sample response has a longer period after N_2 annealing, indicating the shrinkage of the HfO_2 layers. This is confirmed by the TEM image in Fig. 5. Note that the XRR curves of annealed HfO_2 are obviously different from the as-deposited one due to the formation of the Hf-silicate layer and the increase of the interface roughness between each layer, which is obtained by XRR simulation. The HfO_2/SiO_2 interfacial roughness after annealing at 1000 °C for 5 min, which was obtained from the XRR fitting (not shown here), showed an increase of 0.3–0.4 nm as compared to the as-deposited sample. The inset of Fig. 6 is the surface roughness of the HfO_2, which is measured by AFM. The surface roughness of samples increases slightly after PDA [24]. The XRR of the annealed HfO_2 is fitted by the four-layer model (model 2 in Table I) that includes (in sequence): substrate Si, initial chemical oxide layer, Hf-silicate interfacial layer, and HfO_2 [25], and the as-deposited sample is also fitted with the structure without a Hf-silicate layer (model 1 in Table I). Note that although the layer of Hf-silicate is not clearly observed in the TEM picture, a Hf-silicate layer should be reasonably assumed between HfO_2 and SiO_2. Table I lists the corresponding layer thickness T, film density D, and surface roughness R, obtained by XRR fitting, TEM, and AFM. The surface roughness calculated by simulation is quite similar to that obtained from AFM measurement. The interface roughness in TEM is observed in extremely local region on the scale of nanometers. However, the roughness measured by XRR is an average on a large area (in square millimeters). The correlation between TEM roughness and XRR roughness is not known. The error bar of TEM thickness can be roughly estimated from each TEM micrograph. The thickness of the interfacial layer between the Si and the HfO_2 increases significantly when the thin film was annealed at 1000 °C for 5 min (Table I). The oxygen needed for the growth of the interfacial oxide may have originated from the trace oxygen in the flowing N_2 ambient and/or the oxygen in HfO_2 [26].

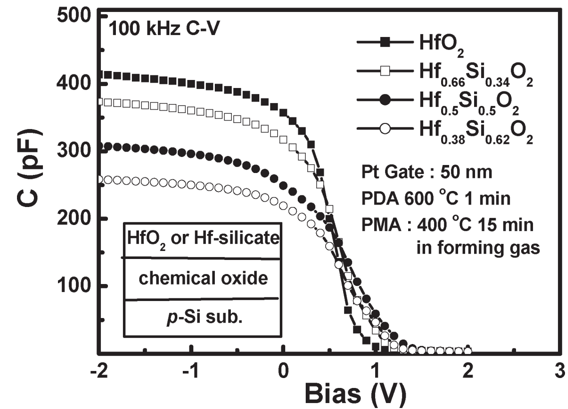

Fig. 7. High-frequency (100 kHz) C–V characteristics of $Pt/HfO_2/Si$ and Pt/Hf-silicate/Si MIS capacitors following PDA at 600 °C for 1 min and PMA at 400 °C for 15 min. The inset shows the device structure. The C–V curve without PMA would be stretched out due to a large number of interface states (not shown).

C. Electrical Properties

The high-frequency (100 kHz) C–V curves measured at room temperature are plotted in Fig. 7; the electrode area

Authorized licensed use limited to: National Taiwan University. Downloaded on February 13, 2009 at 00:47 from IEEE Xplore. Restrictions apply.

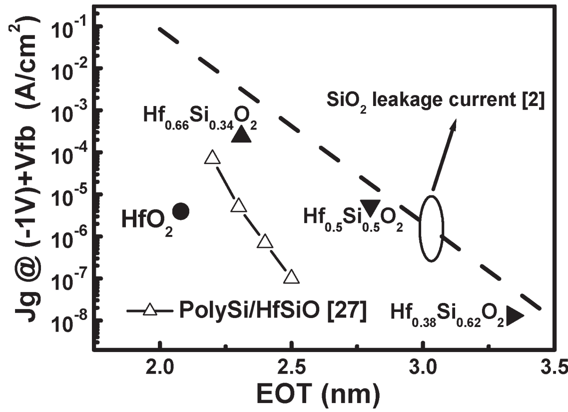

Fig. 8. Relation between leakage current and EOT of the HfO_2 and Hf-silicate devices. The SiO_2 trend line is also shown (dashed line).

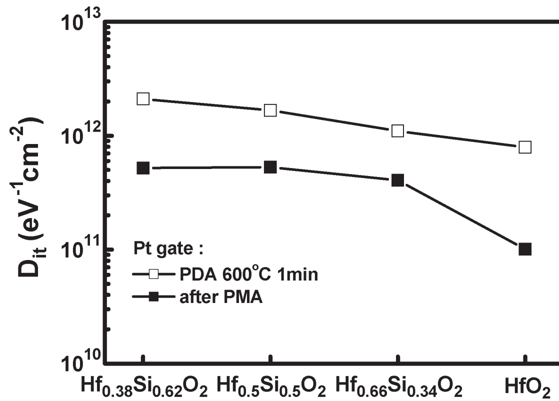

Fig. 9. $D_{\rm it}$ of HfO_2 and Hf-silicate devices with Pt electrodes before and after PMA. The $D_{\rm it}$ value of all high-k samples with PMA is below $10^{12}\ \rm eV^{-1} \cdot cm^{-2}$.

is $2.5 \times 10^{-4}\ \rm cm^2$. The interfacial chemical oxide is grown by SC-1 before the insulator to restrict the interface trap density. The capacitance of the accumulation region increases, indicating an increase in the dielectric constant with increasing Hf concentration (38% to 100%). The gate leakage current density versus EOT of $\rm Hf_xSi_{1-x}O_2$ at a gate voltage of flatband voltage$(V_{\rm FB}) - 1$ for an n-channel metal–oxide–semiconductor diode is shown in Fig. 8. The HfO_2 device shows a $10^4 \times$ leakage current reduction as compared to the SiO_2 device, and the Hf-silicate devices show about one order of magnitude or less leakage current reduction as compared to the SiO_2 device. Note that the relatively larger leakage current as compared to [27] may be due to the larger interfacial layer thickness of our silicate samples. The thinner interfacial layer thickness (1 nm in [27]) with the sample EOT (larger physical thickness of the high-k layer) will thus reduce the leakage current [27], [28]. The interface trap density $D_{\rm it}$ at $V_{\rm FB}$ measured by the high–low (100 and 1 kHz) frequency method is shown in Fig. 9. The $D_{\rm it}$ of these devices is of the order of $1 \times 10^{12}\ \rm cm^{-2} \cdot eV^{-1}$ without PMA and is reduced by about one order of magnitude after a PMA process. The HfO_2 device has the smallest $D_{\rm it}$ both after PMA and before PMA, indicating that the Si in Hf-silicate can create interface defects at the HfO_2/SiO_2 interface.

IV. Conclusion

In summary, we find that the weak FTIR signal from thin $\rm Hf_{1-x}Si_xO_2$ films can be detected by using a "face-to-face" structure. When the HfO_2 thin film on oxide is annealed at high temperature (600 °C and 1000 °C), the formation of a Hf-silicate layer in the HfO_2/SiO_2 interface is evidenced by the occurrence of the FTIR peaks at 960, 900, and 820 $\rm cm^{-1}$, attributed to Hf–Si–O stretching vibrations. Moreover, XPS results also indicate a great signature of the formation of a Hf-silicate layer. The annealed nanomixed HfO_2/SiO_2 sample has the same FTIR peaks, indicating that the nanomixed HfO_2/SiO_2 transformed into Hf-silicate after the thermal process.

Acknowledgment

The authors would like to thank Dr. M. Temple for proofreading this paper.

References

[1] *International Technology Roadmap for Semiconductors*, Semiconductors Industry Association, San Jose, CA, 2001.

[2] Y.-C. Yeo, T.-J. King, and C. Hu, "MOSFET gate leakage modeling and selection guide for alternative gate dielectrics based on leakage considerations," *IEEE Trans. Electron Devices*, vol. 50, no. 4, pp. 1027–1035, Apr. 2003.

[3] C. Hobbs, H. Tseng, K. Reid, B. Taylor, L. Dip, L. Hebert, R. Garcia, R. Hegde, J. Grant, D. Gilmer, A. Franke, V. Dhandapani, M. Azrak, L. Prabhu, R. Rai, S. Bagchi, J. Conner, S. Backer, F. Dumbuya, B. Nguyen, and P. Tobin, "80 nm poly-Si gate CMOS with HfO_2 gate dielectric," in *IEDM Tech. Dig.*, 2001, pp. 651–654.

[4] G. D. Wilk, R. M. Wallace, and J. M. Anthony, "High-k gate dielectrics: Current status and materials properties considerations," *J. Appl. Phys.*, vol. 89, no. 10, pp. 5243–5275, 2001.

[5] R. Choi, C. S. Kang, B. H. Lee, K. Onishi, R. Nieh, S. Gopalan, E. Dharmarajan, and J. C. Lee, "High-quality ultra-thin HfO_2 gate dielectric MOSFETs with TaN electrode and nitridation surface preparation," in *VLSI Symp. Tech. Dig.*, 2001, pp. 15–16.

[6] S. Pidin, Y. Morisaki, Y. Sugita, T. Aoyama, K. Irino, T. Nakamura, and T. Sugii, "Low standby power CMOS with HfO_2 gate oxide for 100-nm generation," in *VLSI Symp. Tech. Dig.*, 2002, pp. 28–29.

[7] R. Chau, S. Datta, M. Doczy, B. Doyle, J. Kavalieros, and M. Metz, "High-κ/metal-gate stack and its MOSFET characteristics," *IEEE Electron Device Lett.*, vol. 25, no. 6, pp. 408–410, Jun. 2004.

[8] P. Punchaipetch, G. Pant, M. A. Quevedo-Lopez, C. Yao, M. El-Bouanani, M. J. Kim, R. M. Wallace, and B. E. Gnade, "Low-temperature deposition of hafnium silicate gate dielectrics," *IEEE J. Sel. Topics Quantum Electron.*, vol. 10, no. 1, pp. 89–100, Jan./Feb. 2004.

[9] W. Zhu, T. P. Ma, T. Tamagawa, Y. Di, J. Kim, R. Carruthers, M. Gibson, and T. Furukawa, "HfO_2 and HfAlO for CMOS: Thermal stability and current transport," in *IEDM Tech. Dig.*, 2001, pp. 463–466.

[10] M.-Y. Ho, H. Gonga, G. D. Wilk, B. W. Busch, M. L. Green, W. H. Lin, A. See, S. K. Lahiri, M. E. Loomans, P. I. Raisanen, and T. Gustafsson, "Suppressed crystallization of Hf-based gate dielectrics by controlled addition of Al_2O_3 using atomic layer deposition," *Appl. Phys. Lett.*, vol. 81, no. 22, pp. 4218–4220, Nov. 2002.

[11] E. Vainonen-Ahlgren, E. Tois, T. Ahlgren, L. Khriachtchev, J. Marles, S. Haukka, and M. Tuominen, "Atomic layer deposition of hafnium and zirconium silicate thin films," *Comput. Mater. Sci.*, vol. 27, no. 1/2, pp. 65–69, 2003.

[12] D.-S. Kil, K. Hong, K.-J. Lee, J. Kim, H.-S. Song, K.-S. Park, J.-S. Roh, H.-C. Sohn, J.-W. Kim, and S.-W. Park, "Development of highly robust nano-mixed $\rm Hf_xAl_yO_z$ dielectrics for TiN/$\rm Hf_xAl_yO_z$/TiN capacitor applicable to 65 nm generation DRAMs," in *VLSI Symp. Tech. Dig.*, 2004, pp. 126–127.

[13] T.-H. Moon, M.-H. Ham, M.-S. Kim, I. Yun, and J.-M. Myoung, "Growth and characterization of MOMBE grown HfO_2," *Appl. Surf. Sci.*, vol. 240, no. 1–4, pp. 105–111, 2005.

Authorized licensed use limited to: National Taiwan University. Downloaded on February 13, 2009 at 00:47 from IEEE Xplore. Restrictions apply.

[14] V. Cosnier, M. Olivier, G. Theret, and B. Andre, "HfO_2–SiO_2 interface in PVD coatings," *J. Vac. Sci. Technol. A, Vac. Surf. Films*, vol. 19, no. 5, pp. 2267–2271, 2001.

[15] C. W. Liu, Y. H. Huang, C. Y. Chen, S. Gurtler, C. C. Yang, Y. Chang, and L. P. Chen, "Infrared studies of laser induced oxide on (100) Si and SiGe layers," *Mater. Chem. Phys.*, vol. 65, no. 3, pp. 350–353, 2000.

[16] N. Rochat, K. Dabertrand, V. Cosnier, S. Zoll, P. Besson, and U. Weber, "Infrared spectroscopy of high-k thin layer by multiple internal reflection and attenuated total reflection," *Phys. Stat. Sol. (C)*, vol. 0, no. 8, pp. 2961–2965, 2003.

[17] D. A. Neumayer and E. Cartier, "Materials characterization of ZrO_2–SiO_2 and HfO_2–SiO_2 binary oxides deposited by chemical solution deposition," *J. Appl. Phys.*, vol. 90, no. 4, pp. 1801–1808, 2001.

[18] Q. Fang, J.-Y. Zhang, Z. Wang, M. Modreanu, B. J. Oullican, P. K. Hurley, T. L. Leedham, D. Hywel, M. A. Audier, C. Jimenez, J.-P. Senateur, and I. W. Boyd, "Interface of ultrathin HfO_2 films deposited by UV-photo-CVD," *Thin Solid Films*, vol. 453/454, pp. 203–207, 2004.

[19] X. Zhao and D. Vanderbilt, "First-principles study of structural, vibrational, and lattice dielectric properties of hafnium oxide," *Phys. Rev. B.*, vol. 65, no. 23, p. 233 106, 2002.

[20] M. Ito, K. Kamiya, M. Hori, and T. Goto, "Subsurface reactions of silicon nitride in a highly selective etching process of silicon oxide over silicon nitride," *J. Appl. Phys.*, vol. 91, no. 5, pp. 3452–3458, 2002.

[21] D. Triyoso, R. Liu, D. Roan, M. Ramon, N. V. Edwards, R. Gregory, D. Werho, J. Kulik, G. Tam, E. Irwin, X.-D. Wang, L. B. La, C. Hobbs, R. Garcia, J. Baker, B. E. White, Jr., and P. Tobin, "Impact of deposition and annealing temperature on material and electrical characteristics of ALD HfO_2," *J. Electrochem. Soc.*, vol. 151, no. 10, pp. F220–F227, 2004.

[22] C. C. Yeo, M. S. Joo, B. J. Cho, and S. J. Whang, "Effect of annealing on the composition and structure of HfO_2 and nitrogen-incorporated HfO_2," *Thin Solid Films*, vol. 462/463, pp. 90–95, 2004.

[23] M.-H. Cho, K. B. Chung, C. N. Whang, D. W. Lee, and D.-H. Ko, "Phase separation and electronic structure of Hf-silicate film as a function of composition," *Appl. Phys. Lett.*, vol. 87, no. 24, p. 242 906, 2005.

[24] R. Ludeke and E. Gusev, "Structural and surface potential characterization of annealed HfO_2 and $(HfO_2)_x(SiO_2)_{1-x}$ films," *J. Appl. Phys.*, vol. 96, no. 4, pp. 2365–2373, 2004.

[25] P. S. Lysaght, P. J. Chen, R. Bergmann, T. Messina, R. W. Mutro, and H. R. Huff, "Experimental observations of the thermal stability of high-k gate dielectric materials on silicon," *J. Non-Cryst. Solids*, vol. 303, no. 1, pp. 54–63, May 2002.

[26] P.-J. Tzeng, S. Maikap, P.-S. Chen, Y.-W. Chou, C.-S. Liang, and L.-S. Lee, "Physical and reliability characteristics of Hf-based gate dielectrics on strained-$Si_{1-x}Ge_x$ MOS devices," *IEEE Trans. Device Mater. Rel.*, vol. 5, no. 2, pp. 168–176, Jun. 2005.

[27] A. Morioka, H. Watanabe, M. Miyamura, T. Tatsumi, M. Saitoh, T. Ogura, T. Iwamoto, T. Ikarashi, Y. Saito, Y. Okada, H. Watanabe, Y. Mochiduki, and T. Mogami, "High mobility MISFET with low trapped charge in HfSiO films," in *VLSI Symp. Tech. Dig.*, 2003, pp. 165–166.

[28] Y. Y. Fan, Q. Xiang, J. An, L. F. Register, and S. K. Banerjee, "Impact of interfacial layer and transition region on gate current performance for high-k gate dielectric stack: Its tradeoff with gate capacitance," *IEEE Trans. Electron Devices*, vol. 50, no. 2, pp. 433–439, Feb. 2003.

Tze Chiang Chen received the B.S. and M.S. degrees in electrical engineering from Chang Gung University, Tao-Yuan, Taiwan, R.O.C., in 1999 and 2001, respectively, and the Ph.D. degree from the National Taiwan University (NTU), Taipei, Taiwan, R.O.C., in 2006.

He is currently with the Department of Electrical Engineering and Graduate Institute of Electronics Engineering, NTU. His research interests are in high-k material, visible light from quantum dots device, and interface properties of semiconductors by MOS tunneling light-emitting diodes.

Cheng-Yi Peng received the B.S. degree in physics from the National Taiwan University (NTU), Taipei, Taiwan, R.O.C., in 2004. He is currently working toward the Ph.D. degree at the Department of Electrical Engineering and Graduate Institute of Electronics Engineering, NTU.

His current research interests include mechanical strained MOSFETs and Ge channel MOSFETs.

Chih-Hung Tseng received the B.S. degree in electrical engineering and the M.S. degree from the National Taiwan University (NTU), Taipei, Taiwan, R.O.C., in 2004 and 2006, respectively.

He is currently with the Department of Electrical Engineering and Graduate Institute of Electronics Engineering, NTU. His research interests include strained Si devices and Schottky barrier MOSFETs.

Ming-Han Liao (S'04) received the B.S. degree in mechanical engineering from the National Taiwan University (NTU), Taipei, Taiwan, R.O.C., in 2002.

Since 2002, he has been with the advanced silicon process group at the Department of Electrical Engineering and Graduate Institute of Electro-Optical Engineering, NTU, where he has been involved in strained Si technology and SiGe-based photonics. He has authored or coauthored more than 30 publications/presentations and has three International Electron Device Meeting papers.

Mr. Liao received the Zhuo Zhang-Zong Scholarship Award in 2005 for his outstanding research work.

Mei-Hsin Chen received the B.S. and M.S. degrees in electrophysics from the National Chiao Tung University, Hsinchu, Taiwan, R.O.C., in 2001 and 2004, respectively. She is currently working toward the Ph.D. degree at the Department of Electrical Engineering and Graduate Institute of Electro-Optical Engineering, National Taiwan University, Taipei, Taiwan, R.O.C.

Her current research interests include electron-injection mechanisms and interfacial chemical reaction in organic light-emitting devices.

Chih-I Wu received the B.S. degree in physics from the National Taiwan University (NTU), Taipei, Taiwan, R.O.C., the M.S. degree in physics from Northwestern University, Evanston, IL, and the Ph.D. degree in electrical engineering from Princeton University, Princeton, NJ, in 2000.

He was with the Component Research Division, Intel Corporation from 2000 to 2004 and was involved in developing advanced semiconductor process technology. He is currently an Associate Professor at the Department of Electrical Engineering and Graduate Institute of Electro-Optical Engineering, NTU. His research interests include organic materials for light-emitting diodes, interface properties of semiconductors, and advanced interconnects and gate stack for nano-scaled CMOS.

Authorized licensed use limited to: National Taiwan University. Downloaded on February 13, 2009 at 00:47 from IEEE Xplore. Restrictions apply.

Ming-Yau Chern received the B.S. degree in physics from the National Taiwan University (NTU), Taipei, Taiwan, R.O.C., in 1984 and the Ph.D. degree in physics from Cornell University, Ithaca, NY, in 1991.

He is currently a Professor of Physics at the Department of Physics, NTU. His research interests are in the synthesis of thin film materials, X-ray crystallography, ellipsometry, transparent conducting oxides, and new nitrides.

Pei-Jer Tzeng (M'03) received the Ph.D. degree in engineering and system science from the National Tsing Hua University, Hsinchu, Taiwan, R.O.C., in 2002.

He is currently with the Electronics Research and Service Organization, Industrial Technology Research Institute, Hsinchu. His current research interests include the fabrication and characterization of MOS devices, gate dielectrics, high-k material, and their application in DRAM and nonvolatile memory.

Chee Wee Liu (M'99–SM'00) received the B.S. and M.S. degrees in electrical engineering from the National Taiwan University (NTU), Taipei, Taiwan, R.O.C., in 1985 and 1987, respectively, and the Ph.D. degree in electrical engineering from Princeton University, Princeton, NJ, in 1994.

He is currently a Professor at the Department of Electrical Engineering, Graduate Institute of Electronics Engineering, and Graduate Institute of Electro-Optical Engineering, NTU. His current research interests include strained Si/Ge, SiGe photonics, Ge/Si on anything, high-k, and metal gate. He invented the first MOS tunneling light-emitting diode/laser diode and photodetectors.

Authorized licensed use limited to: National Taiwan University. Downloaded on February 13, 2009 at 00:47 from IEEE Xplore. Restrictions apply.